ELSEVIER

Journal of Volcanology and Geothermal Research 87 (1998) 117–140

Journal of volcanology and geothermal research

Damage to structures by pyroclastic flows and surges, inferred from nuclear weapons effects

Greg A. Valentine *

Geoanalysis Group EES-5, Mail Stop F665, Los Alamos National Laboratory, Los Alamos, NM 87545, USA

Received 5 May 1998; accepted 6 August 1998

Abstract

In order to define the risk from explosive eruptions, one must constrain both the probability of explosive events and the effects, or consequences, of those events. This paper focuses on the effects of pyroclastic flows and surges (here termed 'pyroclastic density currents', or PDCs) on buildings, infrastructure elements, and to some extent on vehicles. PDCs impart a lateral force to such structures in the form of dynamic pressure, which depends on the bulk density of the PDC (which in turn depends mainly on particle concentration) and its velocity. For reasonable ranges of particle concentration (10^{-3} to 0.5) and velocities (10 to 300 m/s), dynamic pressure on the upstream face of a structure ranges from $\sim$0.1 kPa to 10^{4} kPa. Lateral loads ranging up to about 100 kPa were produced during nuclear weapons tests in the 1940s and 1950s that were designed to study the effects of such loading on a variety of structures for civil defense and emergency response purposes in the event of nuclear war. Although considerable simplifications are involved, the data from these weapon tests provide useful analog information for understanding the effects of PDCs. I reviewed data from the nuclear tests, describing the expected damage from different loadings. Tables are provided that define the response of different structural elements (e.g., windows, framing, walls) and whole structures to loading in probabilistic terms, which in principle account for variations in construction quality, orientation, and other factors. Finally, damage documented from historical eruptions at Mt. Lamington (1951), Herculaneum (AD 79 Vesuvius eruption), and St. Pierre (1902 Mt. Pelee eruption) is reviewed. Damage patterns, combined with estimates of velocity, provide an independent estimate of particle concentration in the PDCs. Details of structural damage should be recorded and mapped around future eruptions in order to help refine this aspect of consequence analysis. Another fruitful approach would be to combine numerical simulations of eruption scenarios, which can produce simulated maps of dynamic pressure, with GIS-based data on structures for a given region; the result would be predictions of consequences that could be used for planning and emergency response training.

Keywords: pyroclastic density currents; pyroclastic flow; pyroclastic surge; structural damage; volcanic hazards

1. Introduction

Explosive volcanic risk assessment involves constraining the probability that explosive eruptions of given sizes will occur within a certain space and time frame, and constraining the consequences of the eruptions. A very large fraction of volcanology research has focused on establishing event probabilities by studying the geologic record at active volcanoes and by monitoring such aspects as seismicity, ground deformation, fumarole discharge, gravity

* Tel: +1-505-665-0259; Fax: +1-505-665-3687; E-mail: gav@lanl.gov

0377-0273/98/$19.00
PII: S0377-0273(98)00094-8

fields, and thermal regimes in order to detect changes in the systems. Work directly related to consequences has been more limited. A first step in consequence analysis for a given volcano is to use its eruptive history as a basis for maps showing the likely distributions of various eruptive products such as debris avalanche, pyroclastic density current (a.k.a. pyroclastic flows and surges; also recognizing that these can be driven by lateral blast in addition to density), fallout, and lahar deposits. These products relate directly to types of damage that could result from their attendant eruption mechanisms. For example, fallout deposits from buoyant eruption plumes result in damage simply from the weight of the deposits, such as roof collapse. Damage from lahars is due to burial of structures in mud and, where the flow is vigorous, to incorporation of material into and transport within the lahar. Pyroclastic density currents (PDCs) cause damage from dynamic pressure exerted on objects, from high temperatures, and by the abrasive power of particles in the currents; quantification of PDC damage from dynamic pressure is the goal of this paper.

Blong (1984) compiled data on the effects (or consequences) of most eruption types on structures, vehicles, and other aspects of society such as agriculture, however, there are few quantitative data on the conditions (pressure, temperature, particle loading) during which damage occurred, particularly for pyroclastic density currents. This is understandable given the harsh conditions within these currents and the unpredictability of their occurrence. Also, until recently our ability to predict conditions within pyroclastic density currents was limited to crude estimates of velocity and qualitative (and often controversial) judgments about particle loading within the currents. The advent of multiphase numerical models of explosive volcanic phenomena (Wohletz et al., 1984; Valentine and Wohletz, 1989; Valentine et al., 1991, 1992; Dobran et al., 1993; Neri and Dobran, 1994; Neri and Macedonio, 1996), coupled with our continually-improving ability to interpret deposits in terms of physical processes (e.g., Sparks, 1976; Wilson, 1985; Freundt and Schmincke, 1986; Fisher, 1990; Druitt, 1992; Palladino and Valentine, 1995; Baer et al., 1997; Bursik et al., 1998), makes it possible to constrain the dynamic conditions in areas affected by explosive eruptions. A goal that is already being pursued by some researchers (Giordano and Dobran, 1994; Dobran et al., 1994) is to model explosive eruption scenarios that produce a range of possible dynamic conditions at points around a volcano. There is a great deal of work remaining to be done to improve the results of these model calculations (for example, multiple particle sizes, better constitutive relations, and moving from two to three dimensions). Nevertheless, we are now at a stage where it is important to begin to quantify the consequences implied by scenario models in order to provide accurate risk assessment.

Because many potentially explosive volcanoes threaten urban regions (e.g., Vesuvius and Campi Flegrei, Italy; Popocatepetl, Mexico; Sakurajima, Japan), an important aspect of consequences is the damage to buildings, infrastructure, and vehicles for a given set of dynamic conditions. Prior knowledge of likely conditions (determined by event probabilities and scenario models of likely events) and resulting damage can aid in mitigation as engineers retrofit existing structures, design new ones that can withstand expected conditions, and by allowing development of evacuation plans that emphasize the most vulnerable areas first in a time of crisis. Similarly, improved knowledge of likely damage is an aid in planning rescue and recovery operations after a disaster.

During the late 1940s and 1950s studies were conducted with the same planning and mitigation goals as described above, but for civil defense in the event of a nuclear attack. By coincidence there is significant overlap in the regime of conditions expected around a nuclear explosion and that which could be experienced during an explosive volcanic eruption. In addition to some data from Hiroshima and Nagasaki, series of tests were done where a range of structures and vehicles were exposed to nuclear explosions at a range of distances from ground zero. This provides us with direct information on structural responses to a range of blast loadings, which can be translated to conditions within pyroclastic density currents. In a sense, some aspects of these nuclear tests are full-scale experiments of volcanic phenomena. In addition to the tests, probabilistic predictions of damage due to nuclear explosions were obtained by a form of expert elicitation; this also provides some information that is useful for

constraining consequences of explosive eruptions to urban areas.

The goal of this paper is to review the observations of damage from nuclear explosions and to glean information that can be combined with numerical scenario models to predict damage from explosive eruptions. The focus is on damage to structures; other critical factors like effects on humans (e.g., Baxter, 1990; Baxter and Gresham, 1997) are not discussed here. I begin by comparing phenomena associated with surface or low-altitude nuclear explosions and explosive volcanic eruptions, emphasizing which aspects of nuclear explosions are within the regime of explosive eruptions and where analogies lie. I then summarize qualitative observations of damage to buildings, and to some extent vehicles and infrastructure elements, from nuclear tests for different ranges of blast overpressure. Probabilistic estimates of damage criteria are reviewed. Finally, I compare damage from nuclear weapons with observations of damage from historical explosive eruptions. Interestingly, damage patterns, combined with independent estimates of velocity, provide a means to estimate particle concentrations in the PDCs. The qualitative consistency between particle concentrations estimated from damage criteria and from independent sedimentological or facies criteria indicate that the use of nuclear blast damage as an analog for PDC damage is sufficiently valid to be useful. Finally, I summarize the implications of this work for volcanic risk assessment and recommend future research.

2. Comparison of nuclear and volcanic explosion phenomena

Our understanding of explosive volcanic eruptions owes a great deal to observations of nuclear explosions, as described by Fisher et al. (1997) in a section aptly titled 'Bikini and the Base Surge' (referring to nuclear tests conducted on Bikini Atoll in the Pacific Ocean). Both types of explosions produce debris-laden plumes that rise rapidly through atmosphere, with large ring vortices at the top of the plume where the ambient air is pushed aside (the *working surface* of Valentine and Wohletz, 1989), until they reach their levels of neutral buoyancy in the atmosphere and spread laterally (termed the *umbrella region* for volcanic plumes; Sparks, 1986). Fallout of particles occurs both from the rising plumes and the umbrella regions. Observations of shallow underwater or underground nuclear explosions resulted in the concept of the base surge, which was fundamental in advancing our understanding of pyroclastic density currents.

2.1. Energy yields

Tremendous quantities of energy are released by both nuclear and volcanic explosions, although there are some important differences in the timing and partitioning of this energy. Nuclear explosion energy yields have ranged up to a few tens of megatons (Mt) of TNT equivalent (one ton of TNT equivalent is 4.2×10^9 J—the traditional 'ton' units are retained when discussing energy yields of explosions); this energy is released in a very short time, on the order of a microsecond. The energy released by nuclear reactions in a weapon raises the temperature of the weapon materials to tens of millions of degrees. The materials then radiate X-rays which are absorbed within a distance of ~ 1 m by the ambient atmosphere, which is in turn raised to a very high temperature. For low-altitude and surface bursts (defined below) this combination of weapon materials (in vapor form) and X-ray-heated air, called the 'fireball', then transmits most of its energy (~ 85–90%) to the surroundings by a combination of thermal radiation and kinetic energy driven as the fireball rapidly expands. The ratio of thermal radiation to air blast energy is about 2:3 in many cases. For comparison, the 18 May 1980 lateral blast at Mount St. Helens had an estimated energy of 24 Mt (Kieffer, 1981), of which 7 Mt was released as the kinetic energy of the expanding cloud. The remaining 17 Mt were released by condensing of steam and cooling of clasts and water droplets (Kieffer, 1981). Given that the total energy released in an explosive eruption is determined by the mass, specific heats, and temperature of erupted material, and that the total volume of the Mount St. Helens blast was only between 0.1–0.2 km^3, we see that explosive eruption energies can be equal to or far in excess of nuclear explosions. Obviously, though, the fact that a nuclear weapon releases all its energy within $\sim 10^{-6}$ s, as opposed

to $1–10^5$ s in an explosive eruption, causes some fundamental differences in phenomena. One major difference is thermal effects; while both types of explosions produce thermal damage, the mechanisms of transport are very different. Heat is transported mainly by thermal radiation from a nuclear explosion, but mainly by advection within density currents in explosive eruptions. This paper focuses on the analogy between nuclear air blast and PDCs, and does not further consider thermal effects.

2.2. Explosion phenomena

In order to more fully constrain where analogies lie between nuclear and volcanic explosions, I now review some of the basic phenomena associated with both. A general, detailed description of weapon phenomena is provided by Glasstone and Dolan (1977) so a brief summary is provided here. The focus is on phenomena associated with low altitude and surface bursts of nuclear weapons. A burst at an altitude of less than 10–15 km, but high enough that the fireball does not touch the ground when it reaches its maximum size, is classified as low altitude, whereas explosions in which the fireball does intersect the ground is a surface burst. In both cases a large portion of the released energy goes into air shock.

The sequence of events in a low-altitude nuclear explosion is illustrated in Fig. 1. First, a high-pressure and -temperature fireball is formed, consisting of vaporized bomb materials and X-ray-heated air (Fig. 1a). The fireball rapidly expands to equilibrate with atmospheric pressure; this expansion drives a strong shock wave (a.k.a. blast wave or air shock) that moves radially away from the fireball (Fig. 1b). Simultaneously, thermal radiation from the fireball rapidly heats the ground surface. If the ground consists of soil (i.e., it is not covered with pavement), any pore moisture rapidly vaporizes, in turn fluidizing the soil to form a dusty layer in the air (Fig. 1b). For low altitude bursts the air shock reflects off the ground surface so that the reflected shock travels back up toward the fireball. Some stress is transmitted into the ground and propagates away from ground zero as a stress wave at a higher velocity than the air shock, due to the higher sound speed of solid rock (Fig. 1c). It is likely that the ground stress wave contributes to the dust layer by acoustic fluidization (Melosh, 1989) of unconsolidated soil. As the fireball expands to achieve pressure equilibrium with the atmosphere it begins to rise due to its buoyancy. As it rises it takes on a rolling toroidal shape and draws air and debris up with it, forming the head and stem of the familiar ‘mushroom cloud’. The rise rates for such clouds can be quite high; for example a low-altitude burst in the megaton range can rise nearly 10 km in the first minute after detonation. The air shock continues to travel away from the original explosion site. The interaction between the primary air shock and the reflected shock produces a vertically-oriented ‘Mach stem’ shock that runs outward along the ground (Fig. 1d). Because of development of the Mach stem, objects on the ground experience a vertical shock and lateral loading even though the burst occurs at some altitude (except in an area immediately beneath the burst, where shock loading will be downward); this is an important point because pyroclastic density currents also will produce lateral loading. Immediately behind the Mach stem, winds, with entrained dust and debris, initially blow outward from ground zero. As the Mach stem travels away from a given location the outward winds are replaced by inward winds due to suction from the rising fireball. After the air shock phenomena are over, the fireball continues to rise and cool until it reaches a neutral buoyancy height. Surface bursts result in a very similar sequence of events, except that the interaction of the fireball with the ground surface results in melting and cratering of the ground, and much more debris from the ground is involved in the rising mushroom cloud (Fig. 1e).

Processes that may accompany the above sequence include base surge and fallout, and the precursor shock. Shallowly buried and surface nuclear bursts may entrain large quantities of dirt and rock, which is lofted to a given height and then collapses to form ground-hugging density currents of gas-particle mixtures. Similar phenomena occur for underwater nuclear explosions where a spray of vapor and droplets is ejected from the sea surface as the fireball erupts from the water. This spray may collapse back and form a density current that moves out across the water. These are true base surges. Note that the ring-shaped cloud of debris observed around the base of low-altitude bursts is typically not a base surge, but is instead the dust layer described in the above

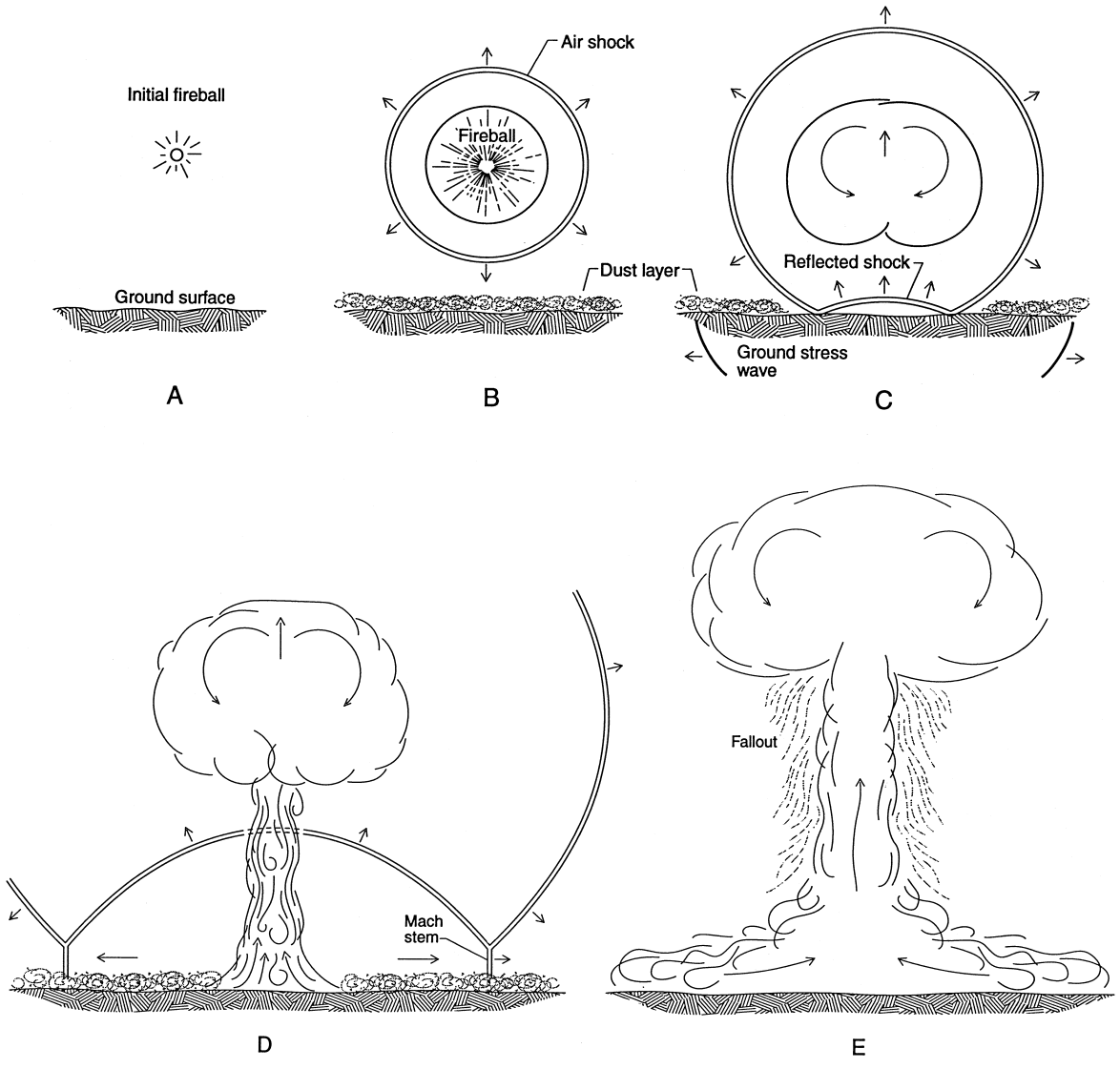

Fig. 1. Sequence of events in a low-altitude nuclear explosion.

paragraph. In some tests where a strong dust layer formed, a shock wave called the 'precursor' was observed to travel ahead of the Mach stem. The mechanisms for formation of the precursor shock are linked to non-ideal conditions (i.e., a hot layer of air near the ground surface) in the atmosphere right above the ground surface. The precursor is not further considered in this paper.

Explosive volcanic eruptions exhibit similar phenomena to nuclear explosions, except that the driving mechanism for air shock processes are the impulse of the eruptive mixture initially entering the atmosphere and the overpressure of that mixture (Fig. 2a), as opposed to an expanding fireball. As the volcanic air shock travels outward, and the eruptive mixture expands, some of the mixture may be pulled laterally by the shock in a 'shock-driven surge', similar to those described by Wohletz et al. (1984)(Fig. 2b). Meanwhile, buoyant portions of the mixture rise vertically as a plume with a mushroom structure. As

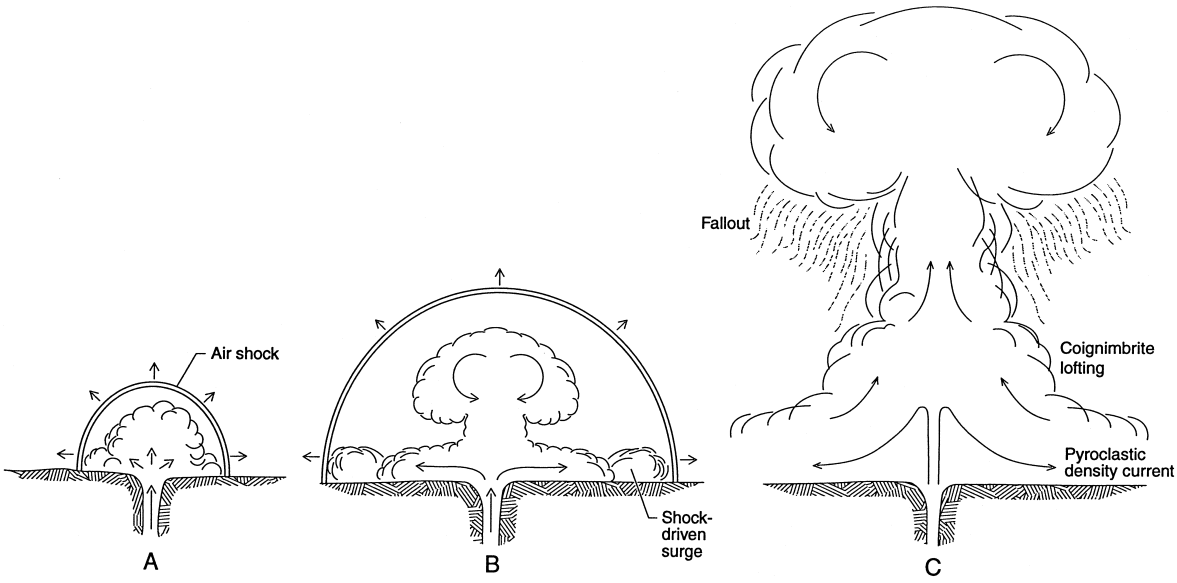

Fig. 2. Sequence of events and main phenomena of explosive volcanic eruptions that produce pyroclastic density currents.

an explosive eruption evolves toward a steady state, the eruptive mixture may collapse to form pyroclastic density currents in a manner very similar to nuclear base surges. The buoyant plume can continue to rise, sucking material back from the top of the PDCs and lofting it to higher altitudes (Fig. 2c; the coignimbrite plume), similar to the continued rise of a nuclear mushroom cloud.

3. Forces on structures

My interest in this paper is in the effects of the above phenomena, with the exception of thermal effects, on human-made structures and vehicles. In both nuclear and volcanic explosions, structures are damaged by a combination of air shock overpressure and dynamic overpressure. To illustrate this, consider a simple structure on the ground, as shown in Fig. 3, at some arbitrary distance from the source of an explosion. The structure initially sits in ambient conditions at atmospheric pressure. The initial air shock, which is vertical even if the explosion was at some altitude due to development of a Mach stem, impinges on the structure. The pressure on the upstream face of the structure is immediately raised to the shock overpressure value plus some additional pressure due to reflection of the shock; this additional pressure rapidly decays back to the shock overpressure value. As the air shock traverses the structure there is a large pressure difference between the upstream and downstream faces, resulting in a net force on the structure that is directed away from the explosion. Responses of structures to this process, termed *diffraction loading* (Fig. 3), depend highly on the surface area of windows and doors, which, once they are blown open, allow propagation of the air shock into the structure and to some degree reduce the loading and resultant damage. For structures with few or no windows, a large pressure difference will suddenly exist between the outside and inside, and the structure may collapse inward if it is still standing after diffraction loading. The length of a structure (measured parallel to the propagation of the air shock) and the shock speed are the main determinants of the duration of diffraction loading. For example, with air shock velocities on the order of 1 km/s (typical of a nuclear blast), a 50 m long structure would experience diffraction loading for 0.05 s.

After passage of the air shock, there is a period during which a strong wind, which may be on the order of 1 km/s or higher near a nuclear explosion, blows outward from the explosion source. This wind

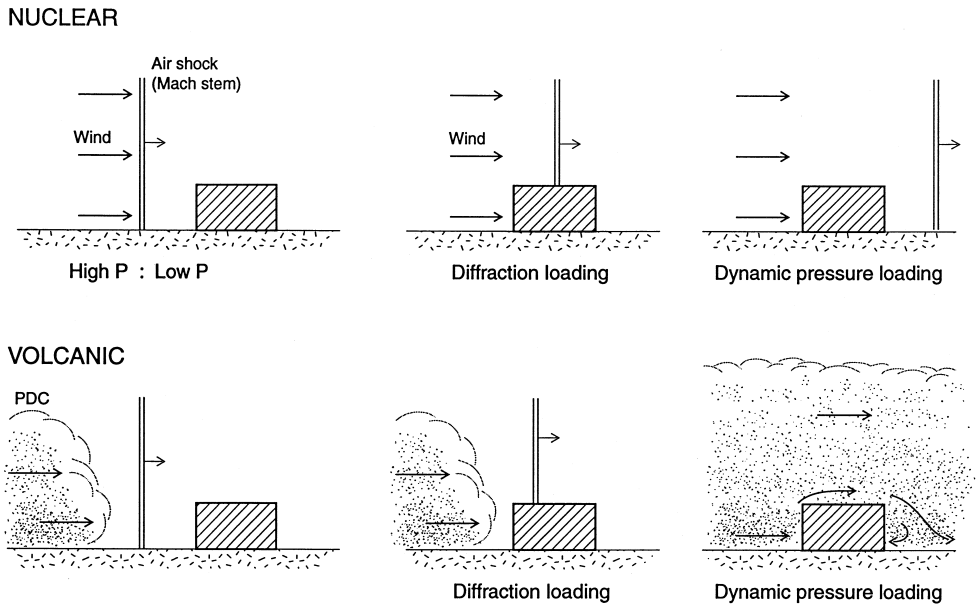

Fig. 3. Mechanisms for lateral loading of a structure on the ground for nuclear and volcanic explosions.

(Fig. 3) exerts a dynamic pressure on the upstream face of a structure as its kinetic energy is converted to a stagnation pressure. Dynamic overpressure (also simply called dynamic pressure in this paper) P_{dyn} is defined as:

$$P_{dyn} = \frac{1}{2}\rho v^2 \quad (1)$$

where ρ is the flow density, and v is the horizontal component of velocity. The effect of dynamic pressure (also called 'drag') loading is the same as diffraction loading in that both cause a net pressure difference across a structure, and thus a downstream directed loading. However, while diffraction loading is for a very short time as the air shock traverses a structure, dynamic pressure can have a much longer duration. For a nuclear explosion the duration of outward-directed dynamic pressure may be as long as a few seconds, before winds reverse due to suction into the rising fireball.

For a volcanic explosion, the main source of dynamic pressure loading will be from pyroclastic density currents (Fig. 3), which, although typically much slower (by an order of magnitude, approximately) than the wind in a nuclear blast, are particle laden and thus denser than the nuclear wind. Dynamic pressure loading from PDCs can have much longer duration than in a nuclear explosion. Dynamic pressures near a nuclear explosion can range as high as a few MPa, but for test conditions for structural effects the dynamic pressures and air-shock overpressures were $10–10^2$ kPa. Dynamic pressures in particle-laden PDCs range from $1–10^4$ kPa, depending mainly on particle loading and velocity (Fig. 4).

There are important differences in the pressure loading of structures in a nuclear explosion compared to those in a volcanic explosion, some of which have already been mentioned. In a nuclear blast at an altitude that maximizes blast damage, the magnitude of overpressure behind the air shock is much larger than that of dynamic pressure when overpressures are less than about 10^2 kPa (Glasstone and Dolan, 1977). As the overpressure increases, dynamic pressure also increases until it is of the same magnitude or even greater than shock overpressure. The details of response of a structure depend on whether it is more sensitive to the very rapid diffraction loading or to the longer-duration dynamic pressure loading. In practice it is difficult to separate the two, since damage from dynamic pressure loading will be affected to some extent by the diffraction load damage as the air shock initially passes over a

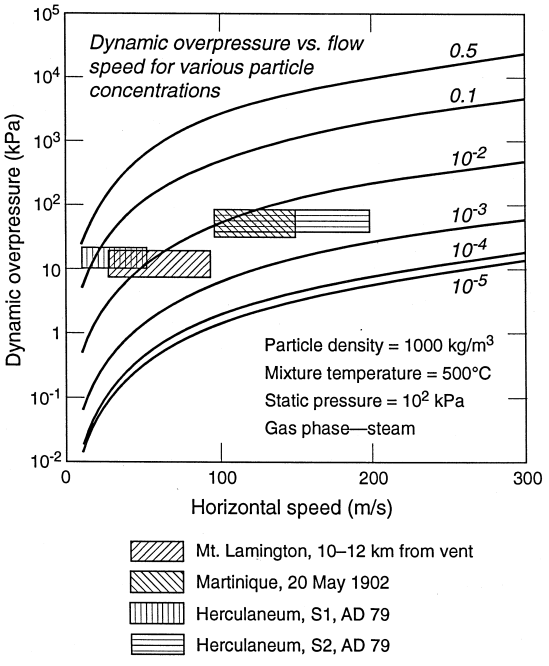

Fig. 4. Plot of dynamic overpressure (see Eq. (1) in text) against horizontal speed for pyroclastic density currents with particle volume fractions of 10^{-5}, 10^{-4}, 10^{-3}, 10^{-2}, 0.1, and 0.5. Mixture density was calculated assuming the gas is water vapor at 10^5 Pa, particles have a density of 1000 kg/m^3 (which accounts for vesicularity), and the PDC temperature is 500 C. These are representative conditions for many PDCs. Note that the parameter that has the largest affect on dynamic pressure (for a given velocity) is particle density—larger particle densities would shift the curves upward, and lower densities would shift it downward, in proportion to the actual density assumed. Boxes show inferred conditions within selected PDCs based on observed damage patterns and independent velocity estimates.

structure. For explosive eruptions it is unlikely that the air shock will be sufficiently strong to cause structural damage except very close to the vent, therefore, reducing the importance of diffraction loading, while subsequent dynamic pressure loading could be quite high (Fig. 4) and for a long duration (the duration of the PDC), as discussed above. Also, for long-duration PDCs the effective shape of a structure may be modified during an eruption (even if it is not damaged early on) by deposition of pyroclastic material around it. The data on structural damage from nuclear tests are commonly given simply as a function of peak overpressure behind the air shock, which reduces the direct applicability of the data to explosive volcanic data (in addition to lumping diffraction and dynamic pressure loading together for the nuclear data themselves). Nevertheless, the nuclear tests provide the nearest to full-scale experimental data that can be applied to volcanic effects that I am aware of. Although there is a great deal of simplification involved, I take the approach of using the air shock overpressure values of nuclear tests as analogous for the dynamic overpressure effects of PDCs. As stated above, both ultimately cause a net lateral force on a structure, the main difference being the time scale of the loading. This simplification is most appropriate for buildings that are of sufficient size to experience significant diffraction loading while the air shock traverses the structure, and is less appropriate for vehicles and narrow structures (e.g., poles, smoke stacks) that are most susceptible to dynamic pressure loading.

One can easily conclude that the response of structures at a given location to loading from nuclear and volcanic explosions depends in detail on many variables in addition to the mechanism of loading (diffraction or dynamic pressure). These include the shape of the structure, its orientation relative to propagation of blast phenomena, the number of openings in the structure, and whether it is a framed, masonry, or reinforced design. The next section focuses on the results of nuclear weapons effects tests that addressed these factors for a range of structures at various blast loadings. However, even for buildings of the exact same design there will be variations in their responses due to varying quality of workmanship and materials. In most cities where there is explosive volcanic risk it will not be practical to quantify the mechanical properties of each existing and planned building. A similar problem presented itself to civil defense planners trying to quantify the risk from nuclear attack scenarios in cities. This led to development of probabilistic approaches based on an early form of expert elicitation (e.g., Pickering and Bockholt, 1971), which are also described and applied to volcanic scenarios below.

4. Description of weapons effects tests and results

During the early phases (1945–1963) of the nuclear arms race between the USA and the USSR,

military and civil defense agencies felt a great urgency in the need to minimize the loss of life, infrastructure, and shelter in the event of an attack and to plan effective emergency response. As a result numerous nuclear tests were conducted to constrain the responses of various structures, including houses, industrial buildings, hardened shelters, railways, and bridges, and vehicles to blast conditions. Many of these tests for the USA occurred in the mid-1950s at the Nevada Test Site in 'Operation Teapot'. Other such tests were conducted at Bikini Atoll during 'Operation Greenhouse' and other test series (e.g., Hayen, 1952). Many of the data from these tests have been declassified during recent years, although the reports are often difficult to obtain. Many results below are summarized directly from these reports. Glasstone and Dolan (1977) provide a very readable and comprehensive review as well. After ratification of the Nuclear Test Ban Treaty in 1963, most nations' testing programs moved to a strictly underground approach with the goal of containing all explosion products below the surface in the immediate vicinity of the test. This marked the permanent end of effects testing with civilian structures. By that time the number of weapons and their individual yields (up to several Mt) had moved the arms race into the regime of Mutually Assured Destruction, rendering the survivability of civilian structures more or less a moot point.

For the weapon effects tests discussed here, structures and vehicles were set up at various distances from ground zero, each distance representing a certain value of air shock overpressure. Many of the test data summarized below are associated with detonation of the Apple II device (30 kt yield) on the top of a 150 m high tower at the Nevada Test Site. In addition some observations from Hiroshima and Nagasaki are included because these provide the only data on large buildings typical of urban areas. In these two cases observations have been typically reported as functions of distance from ground zero. I converted this to shock overpressure values (focusing only on the regions where Mach stem development would have resulted in lateral loading on structures) using the approach laid out in Chapter 3 of Glasstone and Dolan (1977) with the estimated yield and height of burst of these two explosions. Because of the many simplifications involved in using these test data as analogs for explosive volcanic effects, I summarize only the general results of the tests and observations on various structural types and at several overpressures (pressures are given in units of psi, pounds per square inch, in addition to SI units to aid in cross-referencing the literature—1 psi = 6.9 kPa). Fig. 4 captures most of the range of dynamic overpressures that could be expected in pyroclastic density currents. The reader is referred to the original reports and to Glasstone and Dolan (1977) for more details.

4.1. Damage at 7–14 kPa (~ 1–2 psi)

Low-concentration pyroclastic density currents traveling faster than about 100 m/s, or high-concentration PDCs with velocities as low as ~ 10 m/s are capable of producing dynamic overpressures of the order of 7 kPa (Fig. 4). Overpressures of this magnitude represent the onset of structural damage around nuclear explosions. Reinforced concrete buildings, whether multi- or single-story, suffer little if any structural damage at these loadings; however, glass windows, false ceilings and interior partitions can be heavily damaged as the air shock propagates into the building. If the ratio of window area to wall area is sufficiently high to allow flowage of a PDC into such a building, similar damage might be expected in a volcanic scenario. Heavily steel-framed buildings may survive loadings of the 7–14 kPa range, although light wood or aluminum wall panels may be destroyed or bent on the upstream face of a building (Johnston, 1956). Light steel-framed buildings, however, may experience severe structural damage as the frame bends under loading (Fig. 5).

Houses suffer varying damage in this overpressure range. Masonry and precast concrete houses suffer little or no structural damage, but windows and doors were blown out and some window frames can be partially ripped from their walls (Randall, 1961). Wood frame houses suffer more serious damage. In addition to severe window and door damage, roof beams and floor supports begin to break at around 10 kPa overpressure. Weakly built wood frame houses begin to lean in the downwind direction.

Most heavy infrastructure elements, such as roads and railways, are not appreciably damaged by this

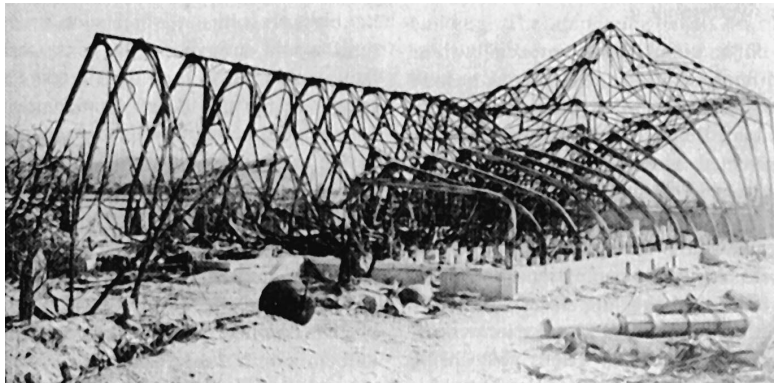

Fig. 5. Damage to a single-story, light steel-frame building in Hiroshima (1.3 km from ground zero). This structure was exposed to an overpressure of about 12 kPa. Some of the collapse of the structure was due to fire after the blast damage (such fires would also be expected after passage of sufficiently hot pyroclastic density currents). From Glasstone and Dolan (1977).

overpressure range. In a volcanic scenario, these structures could be covered with debris and pyroclastic deposits, but would be useable as soon as they were cleaned off. Areal power and telecommunications lines may be damaged, adding difficulty to local response and recovery work. Vehicles, including trains, exposed to these overpressures suffer minor damage in the form of broken windows and bent body panels, but typically are still operable and could be used for emergency operations.

4.2. Damage at 20–30 kPa (~ 3–4 psi)

PDCs with particle concentrations of 10^{-2} and velocities greater than about 50 m/s (and lower velocities for higher-concentration PDCs) are capable of producing dynamic overpressures in this range, resulting in moderate to severe damage. Steel-frame buildings with light walls (e.g., aluminum, wood, or sheet rock) suffer damage in this overpressure range as wall panels are blown off (particularly on the upstream face), and the steel frame itself is bent and even pulled out of concrete footings (Fig. 6). However, if wall materials blow off or fragment very quickly, reducing the load on the frame, it is possible for the frame itself to suffer little damage so that it might be re-used or walled in for emergency shelter. Buildings made of self supporting aluminum or light steel panels (common as storage buildings) bend downwind and collapse at these overpressures, rendering them useless, although heavy, corrugated steel buildings that are strongly bolted together will buckle but remain standing (Johnston, 1956). Most framed, reinforced, multistory concrete buildings suffer sufficient damage that they would require demolition and rebuilding, as the upstream-facing walls lean inward and begin to collapse, and roofs collapse.

Typical wood-frame houses are damaged beyond repair in this range of overpressure. For nuclear explosions in Nevada in 1955 (Randall, 1961), some techniques for reinforcing such houses were applied to test how they affected the house's survivability (in this case a simple two-story house). These techniques included reinforced concrete basement/foundation walls, heavier connections between structural elements, larger boards for rafters and wall studs, and use of plywood for interior wall and ceiling panels instead of lath-and-plaster. Although this reinforced structure remained standing after exposure to 30 kPa, it was so severely damaged that it was not reusable. The roof was collapsed and blown off, the front wall was dished in, and part of the brick chimney was blown off. Most joists and beams were severely cracked. The experience of Nagasaki and Hiroshima show that in this overpressure range most wood frame houses simply collapse.

Damage to heavy infrastructure from this range of overpressure is expected to be slight to moderate, although it is difficult to find direct data on this. Train cars begin to be seriously damaged as their walls crack and partially blow off. It is likely that cars and trucks would be significantly displaced and

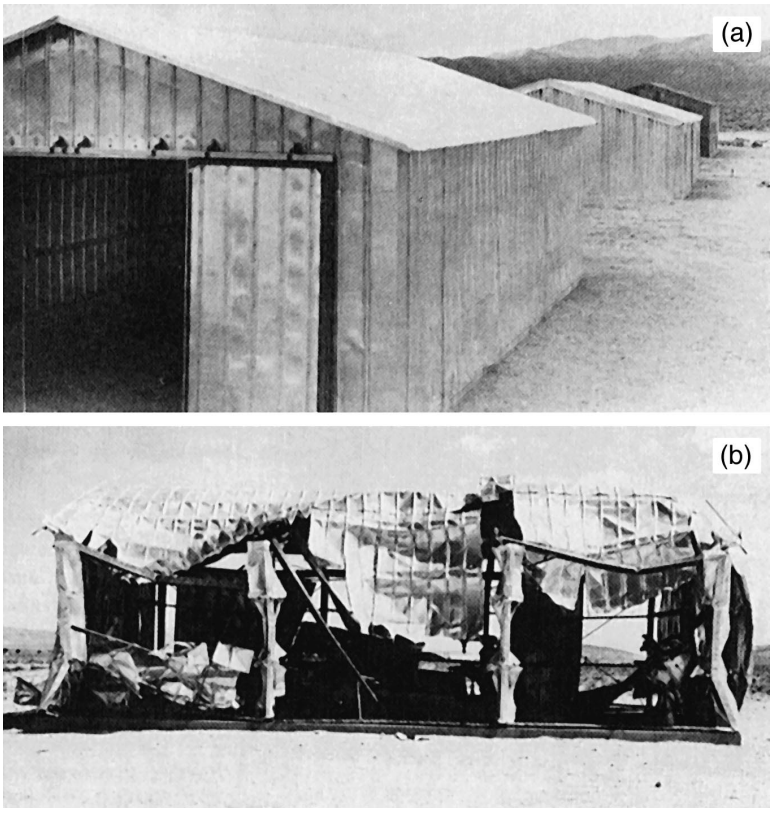

Fig. 6. Rigid steel frame building with light walls before (a) and after (b) exposure to overpressure of 21 kPa. From Glasstone and Dolan (1977).

rolled, but most would still be operational (but not pretty).

4.3. Damage at ≥ 35 kPa (~ 5 psi)

The lower bound of this overpressure range marks the onset of essentially total destruction for most buildings. A pyroclastic density current with particle concentration of 0.01, traveling at a speed of about 80 m/s is capable of producing 35 kPa dynamic overpressure. However, PDCs with concentrations between 0.1–0.5, which may be typical of flows that produce high-aspect ratio ignimbrites, produce such dynamic overpressures at relatively low velocities of 10–20 m/s.

Data on the response of multistory buildings mainly come from Hiroshima and Nagasaki. Some reinforced-concrete frame buildings in those cities survived the 1945 bombings even at overpressures higher than 35 kPa; these buildings had been designed to be earthquake resistant (limited to ~ 30 m in height and capable of withstanding lateral loads up to 10% of the vertical load of the structure). However, even in these cases the windows and doors were blown out and the interior was extensively damaged. I expect that similar damage would happen during the extreme conditions of PDC being considered here. Cities that are vulnerable to explosive eruptions also tend to have significant earthquake hazards and therefore are expected to have at least some buildings that are designed to resist earthquakes. During a volcanic crisis these buildings would be most likely to maintain their structural integrity, so that they could be used for emergency shelter if windows and doors can be sufficiently strengthened or covered. More typical reinforced-concrete frame buildings were damaged beyond repair in Hiroshima and Nagasaki, as illustrated in

Fig. 7. Steel frame structures lean downwind and partially or completely collapse at overpressures exceeding 35 kPa.

The only type of house that has been observed to survive overpressures of 35 kPa are single-story, low profile buildings with walls of precast concrete slabs or blocks. In the Nevada test reported by Randall (1961) such structures had flat roofs made of 15 cm-thick precast concrete. As expected, windows and doors are blown off, but there is little if any structural damage. Such structures would make good emergency response coordination centers and could provide storage for food rations. However, in an eruption scenario where pyroclastic density currents may occur, these low-lying buildings, while being relatively sturdy against the lateral load, could also be quickly buried or partially buried by a sustained PDC.

Most personal vehicles exposed to 35 kPa overpressures can be expected to be damaged beyond any use. Heavy trucks will be seriously damaged at this overpressure but still useful for emergency response (Shaw and McNea, 1957); however, after exposure to any higher overpressures even most heavy duty trucks would not be driveable. Empty railway cars were blown off their tracks at about 41 kPa overpressure in a Nevada test. A heavily loaded railroad car suffered severe damage to its walls and roof, but remained on the tracks and could be hauled away after 41 kPa overpressure, but at 51 kPa it was blown off the tracks and at 62 kPa it was completely destroyed (Glasstone and Dolan, 1977). A diesel train engine exposed to 51 kPa remained operable. In the same test electrical equipment including utility poles, suspension towers, and transformers were exposed to overpressures up to 35 kPa. Some towers and poles were knocked over, but most remained standing, such that moderate repairs could restore the system. However note that these types of structures are relatively unaffected by diffraction loading because their members are narrow. Instead, they are most sensitive to dynamic pressure loading which in this case only amounted to about 4 kPa. Therefore I expect that in a volcanic scenario such structures would be effectively destroyed by the higher dynamic pressures of most PDCs. At these, and potentially at lower overpressures water pipes in building walls or that extend above the ground tend to be ruptured. At Nagasaki this resulted in a dramatic loss of water pressure in the city supply system, severely reducing the ability of emergency responders to put out fires caused by the explosion—a similar situation could easily arise in a volcanic scenario. Heavy infrastructure elements such as reinforced bridges begin to buckle and experience significant damage at overpressures above about 100 kPa.

4.4. Failure of individual structural elements

Glasstone and Dolan (1977) briefly discuss the overpressure conditions for failure of individual structural elements of common buildings. Although they focus on elements that are sensitive to air shock overpressure, implying that they can endure little

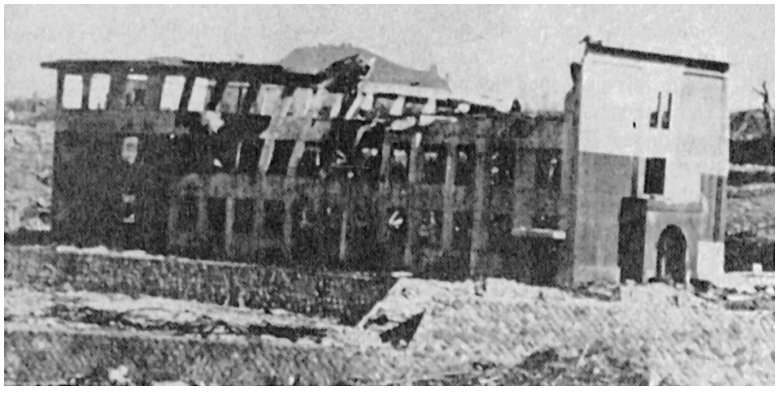

Fig. 7. Three-story, reinforced-concrete frame building in Nagasaki after exposure to overpressure of about 31–35 kPa (0.66 km from ground zero). Note partial collapse of the facing, upstream wall. From Glasstone and Dolan (1977).

Table 1
Conditions of failure of overpressure-sensitive structural elements[a]

Structural element	Failure	Approximate side-on peak overpressure (kPa)
Glass windows, large and small.	Shattering usually, occasional frame failure.	3.4–6.9
Corrugated asbestos siding.	Shattering.	6.9–13.8
Corrugated steel or aluminum paneling.	Connection failure followed by buckling.	6.9–13.8
Brick wall panel, 8 in. or 12 in. thick (not reinforced).	Shearing and flexure failures.	21–69
Wood siding panels, standard house construction	Usually failure occurs at the main connections allowing a whole panel to be blown in.	6.9–13.8
Concrete or cinder-block wall panels, 8 in. or 12 in. thick (not reinforced).	Shattering of the wall.	10.3–38

[a]Glasstone and Dolan (1977).

plastic deformation, these conditions probably roughly apply to dynamic overpressures that might be experienced in pyroclastic density currents. Table 1 provides these failure conditions. This information is included here because it may be useful for determining which structural elements to reinforce in a city that is preparing for a potential explosive eruption.

4.5. Damage to forests

Glasstone and Dolan (1977) also tabulate criteria for the damage of forests, which is here modified to show forest damage for different dynamic overpressures (Table 2). Comparing the criteria in Table 2 with dynamic overpressures for pyroclastic density currents (Fig. 4) we see that nearly complete blowdown of a forest can occur with dynamic pressures as low as 2 kPa, which corresponds to ~ 70 m/s for a dilute (10^{-3} solid concentration) current. Note that these criteria are generalized and there will be some variations depending on the types of trees and their shapes.

5. Probabilistic approaches

As stated earlier, variations and uncertainties in building properties (e.g., orientation, quality of workmanship), along with the limited nature of tests and observations of damage from nuclear weapons (as with explosive eruptions), suggest that a probabilistic approach to damage as a function of overpressure would be useful. Pickering and Bockholt (1971) produced a very useful set of probabilistic damage criteria for a range of structures based on an early form of expert elicitation. First, the authors conducted a thorough review of the literature on blast damage to structures and structural elements of interest (selected according to their importance in

Table 2
Damage criteria for forests[a]

Damage type	Nature of damage	Dynamics overpressure (kPa)
Severe	Up to 90% of trees blown down; remainder denuded of branches and leaves. (Area impassable to vehicles and very difficult on foot.)	2–2.4
Moderate	About 30% of trees blown down; remainder have some branches and leaves blown off. (Area passable to vehicles only after extensive clearing.)	1–1.2
Light	Only applies to deciduous forest stands. Very few trees blown down; some leaves and branches blown off. (Area passable to vehicles.)	0.5–0.8

[a]Glasstone and Dolan (1977).

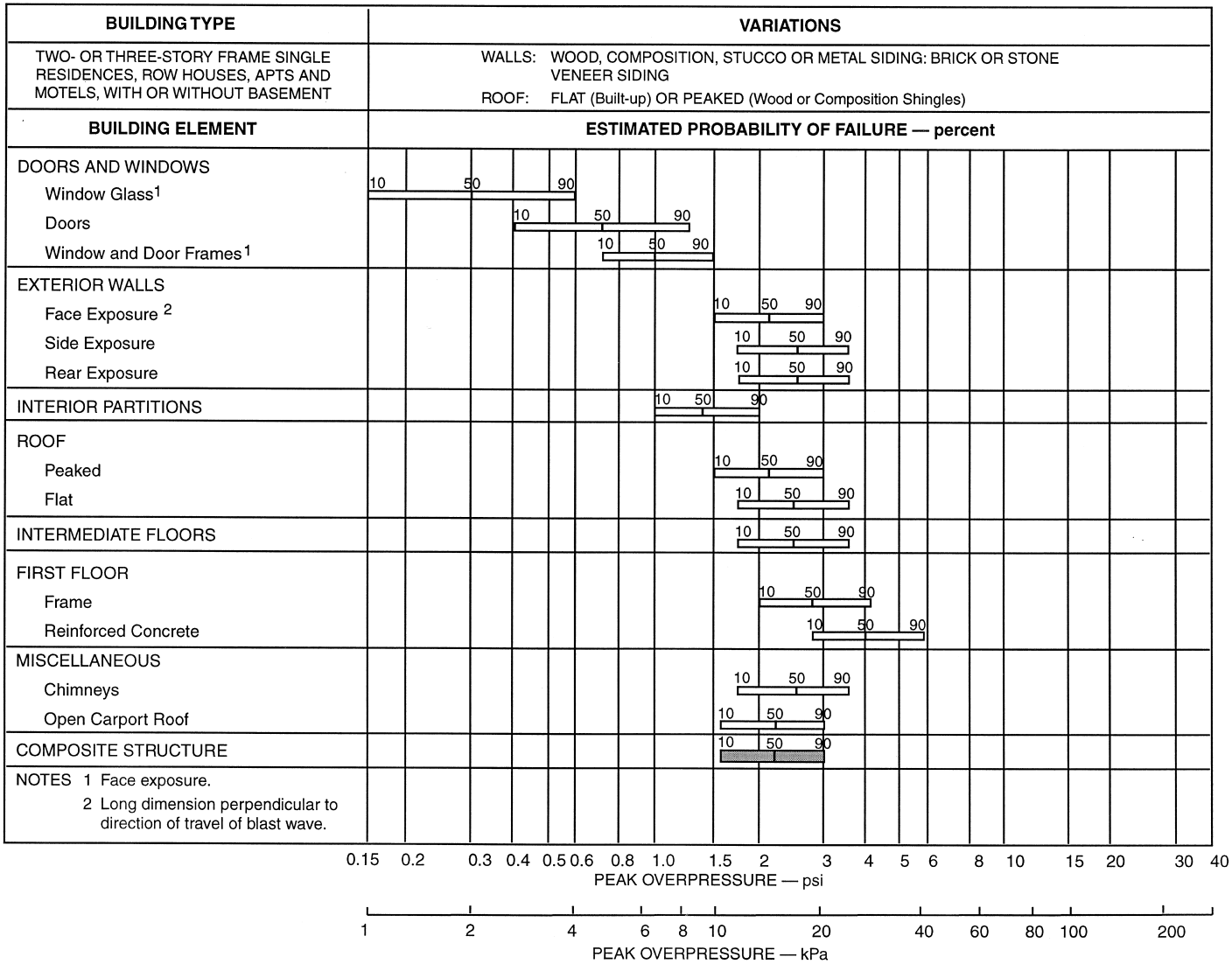

Fig. 8. Estimated probability of failure chart for two- or three-story frame single residences, row houses, apartments, and motels. Modified from Pickering and Bockholt (1971).

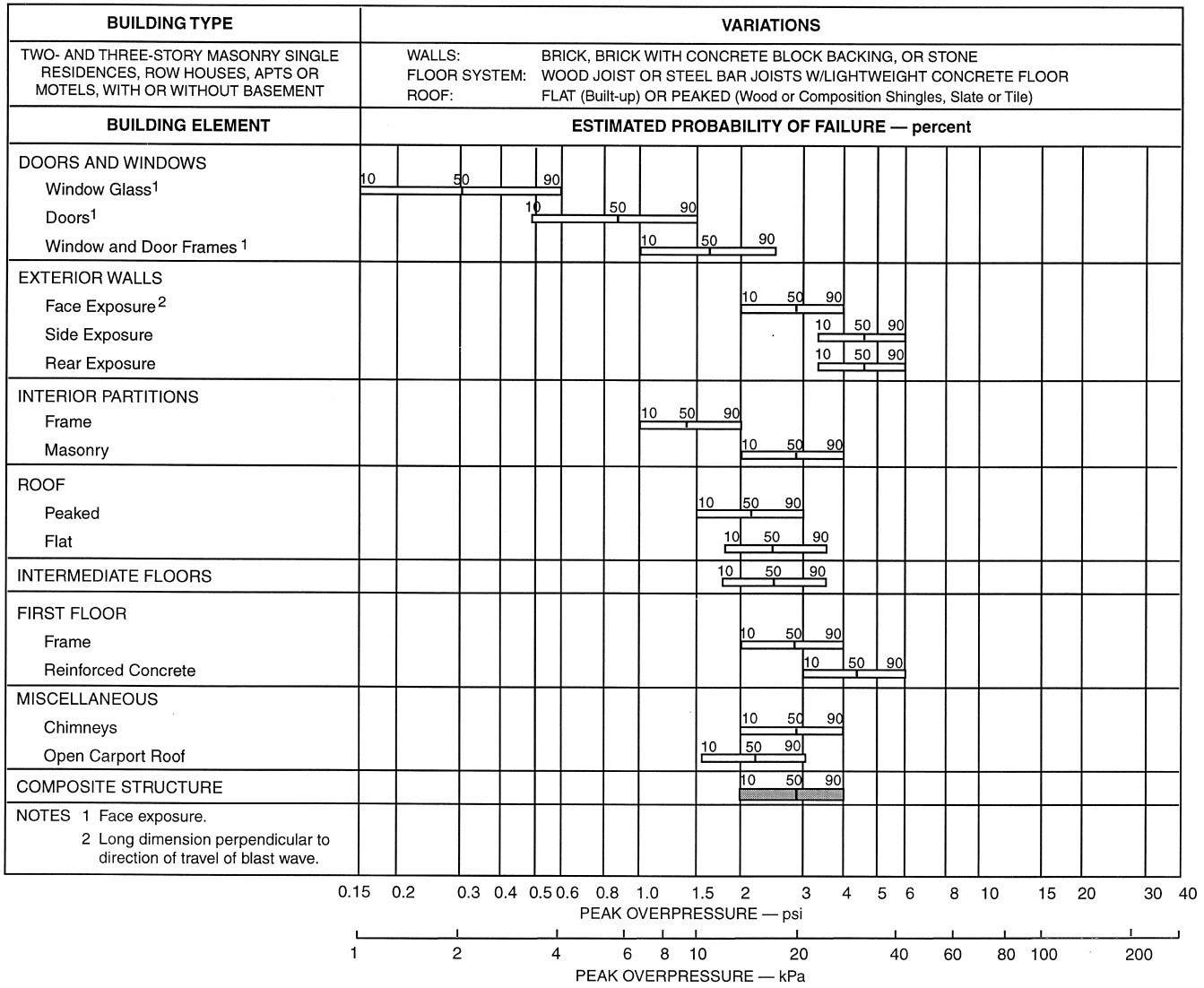

Fig. 9. Estimated probability of failure chart for two- and three-story masonry single residences, row houses, apartments, or motels. Modified after Pickering and Bockholt (1971).

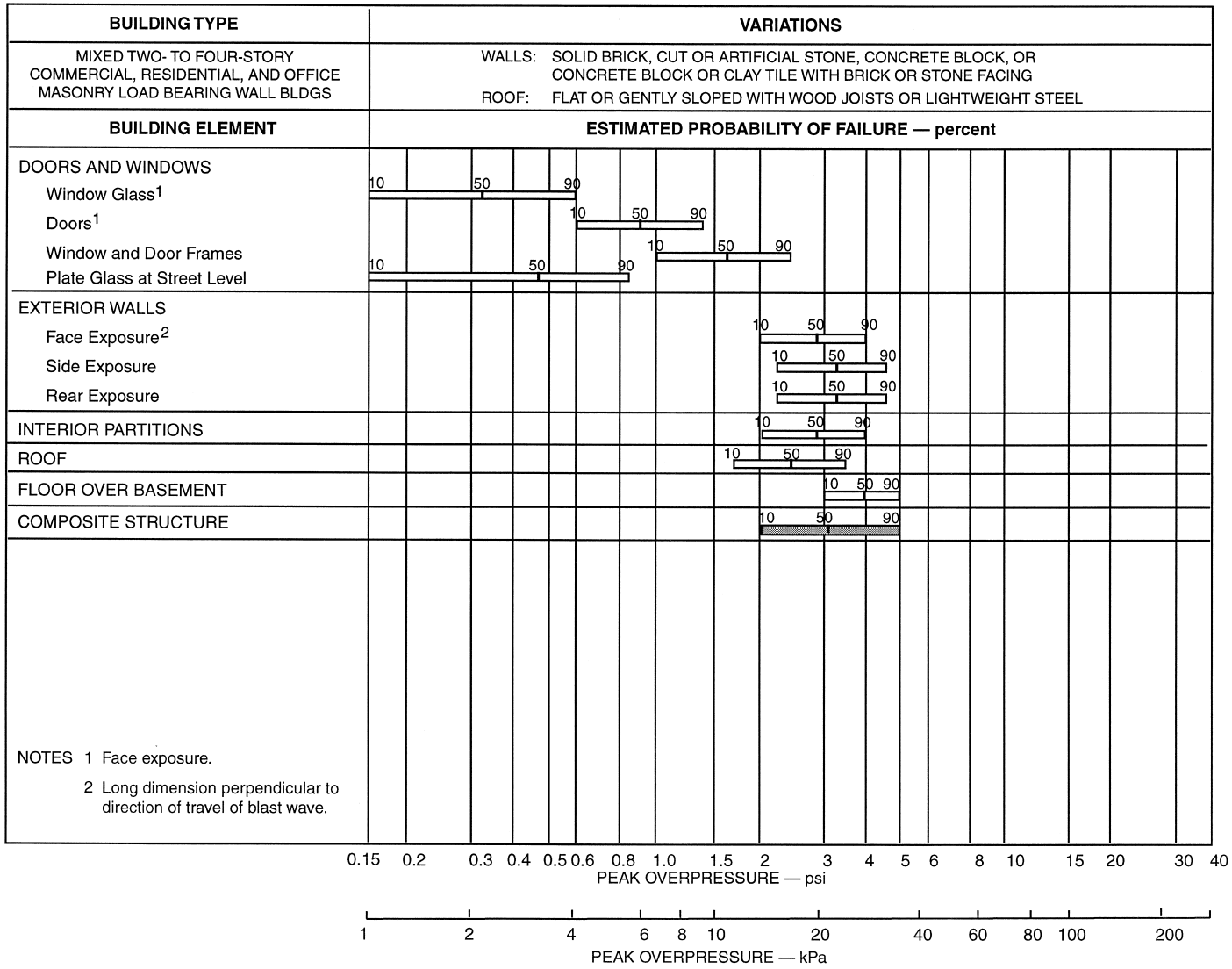

Fig. 10. Estimated probability of failure chart for mixed two- to four-story commercial, residential, and office masonry buildings with masonry load-bearing walls. Modified after Pickering and Bockholt (1971).

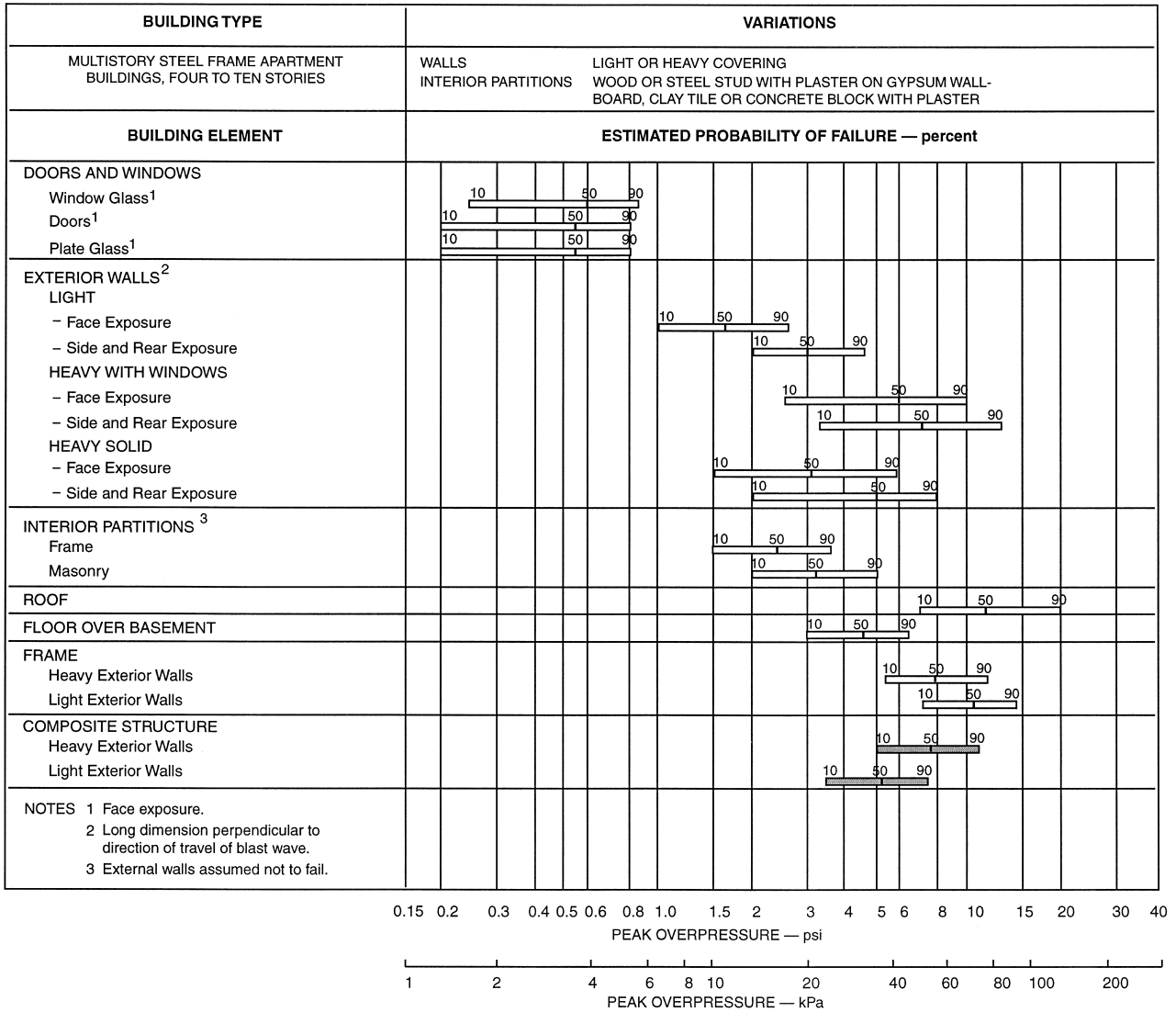

Fig. 11. Estimated probability of failure chart for multistory steel frame apartment buildings, four to ten stories high. Modified after Pickering and Bockholt (1971).

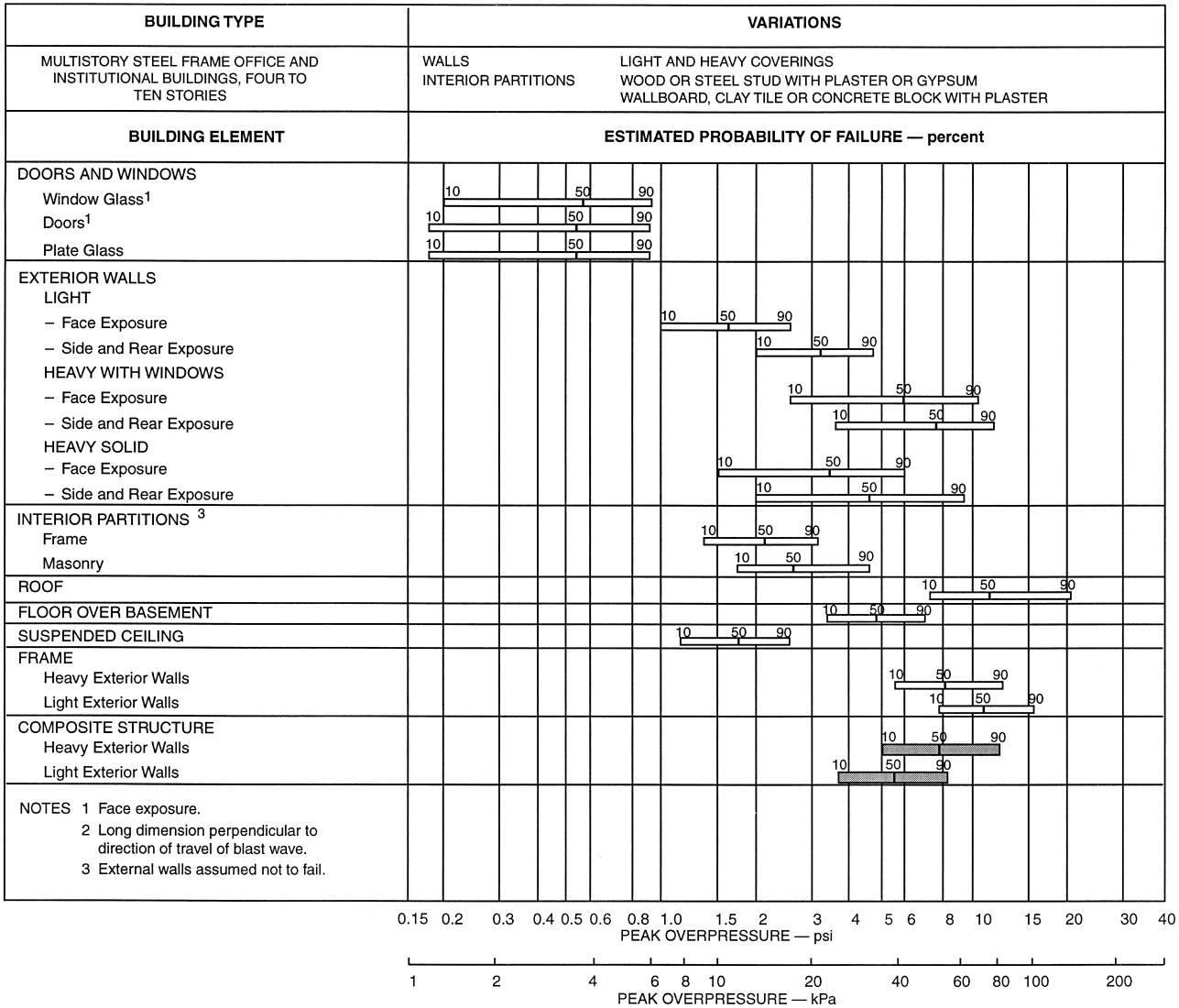

Fig. 12. Estimated probability of failure chart for multistory steel frame office and institutional buildings, four to ten stories high. Modified after Pickering and Bockholt (1971).

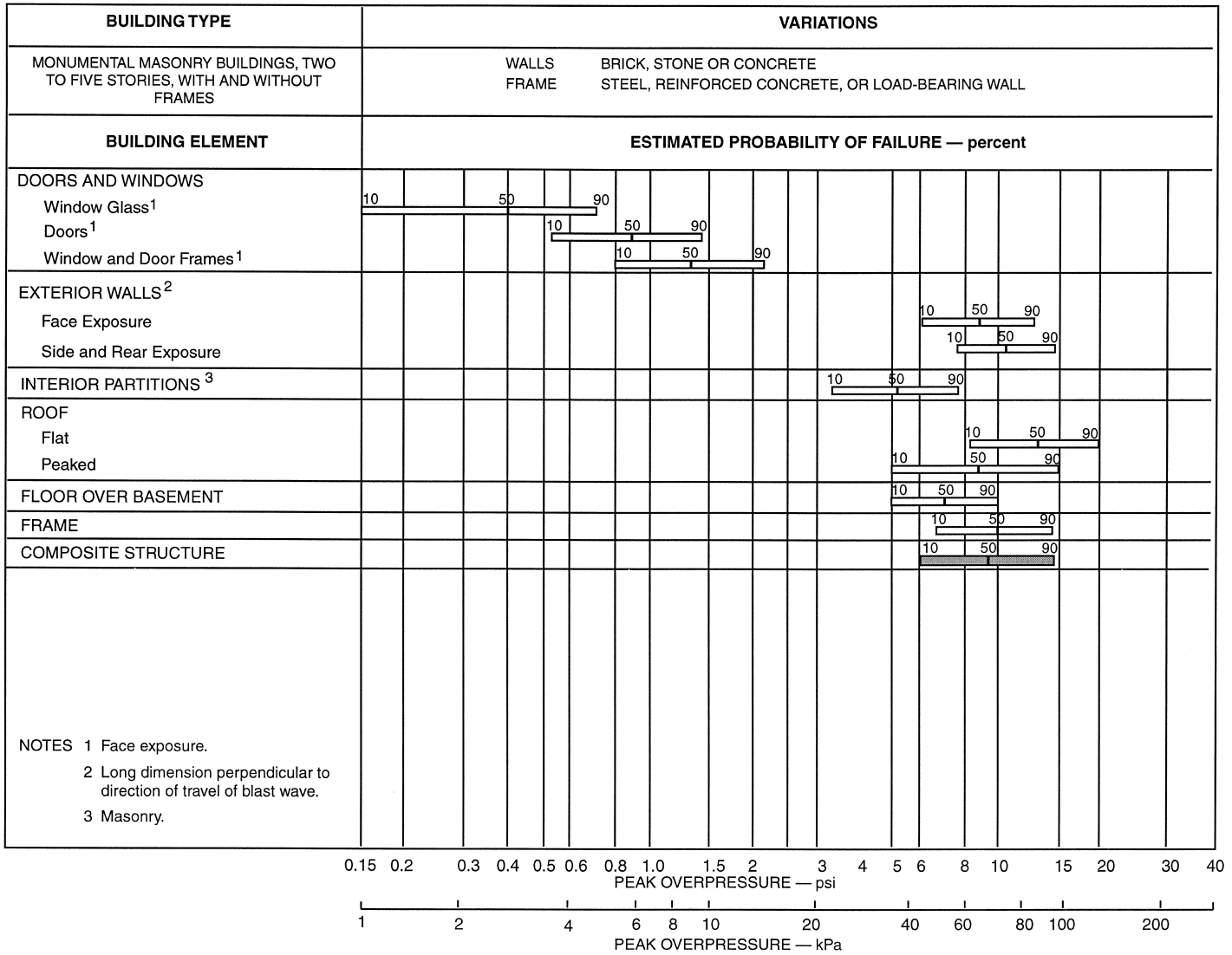

Fig. 13. Estimated probability of failure chart for monumental masonry buildings, two to five stories high. Modified after Pickering and Bockholt (1971).

urban settings). Based on this literature review, the overpressure values at which there is a 10%, 50%, and 90% probability that a given structure will fail ('failure' implies damage beyond repair and collapse) were estimated and probability distributions were developed based on these estimates. These distributions were then reviewed and critiqued by engineers with direct experience in experimental and analytical studies of nuclear blast damage to buildings; the distributions were modified to address the reviews as appropriate. In addition, for each structure type included in the study, the same type of estimates were done for the main structural elements (e.g., facing wall, roof) of that type.

Charts showing these damage criteria for selected building types, along with details of the construction of the buildings, are shown in Figs. 8–13. For each building type, all of the main elements (e.g., windows, walls, roof) have an estimated range of failure overpressures. Fig. 8, for example, shows that the upstream exterior wall (face exposure) of that type of building will have a 10% probability of failing at about 10 kPa (1.5 psi), a 50% failure probability at ~15 kPa (2.2 psi), and a 90% probability of failure at ~21 kPa (3 psi). Combined with the damage observations reviewed in the sections above, these charts provide a means for estimating the extent and probability of damage at a given location given a predicted range of dynamic overpressure and some prior knowledge of building types.

6. Comparison with documented damage from explosive eruptions

I am aware of few descriptions of the details of structural damage from pyroclastic density currents. In this section, I summarize some observations of damage, discuss the PDC conditions implied by the damage, and, where reasonable, compare with independently-estimated conditions within the currents. If eruptions that damage developed areas occur in the near future it would be useful for PDC effects to be mapped in terms of degree of damage for various structure types and to attempt to correlate these data with calculated or observed flow conditions. An interesting side application of this work is that given independent estimates of velocity, along with a given type of damage, one can estimate a range of particle concentrations in a pyroclastic density current. The broad consistency between particle concentration estimated from the damage framework described above, and that estimated by sedimentological or facies arguments, indicates that the nuclear blast damage criteria are useful analogs for qualitative prediction of PDC-induced damage. This is particularly true for PDCs that are of relatively short duration (seconds to tens of seconds), which is likely true for the cases described below, where the time scale of lateral loading is not too different from that around a nuclear explosion.

6.1. 1951 Mt. Lamington eruptions

Taylor (1958) provided a detailed account of the 1951 eruptions at Mt. Lamington, Papua, which included dome-building and explosive phases and the formation of pyroclastic density currents (nuees ardentes) during the climactic eruption on 21 January. The area affected by these PDCs included many agricultural villages. Buildings in these villages apparently were mainly wood frame houses, many on stilts rather than on the ground, that were completely destroyed by the PDCs. Exceptions to this were: (1) an District Commissioner's building and three steel huts located at Higaturu, about 10 km north from the active vent, and (2) Sangara Mission, about 1.5 km down-slope of Higaturu.

At Higaturu, the District Commissioner's building (house) was a U-shaped building, pointing in the downflow direction. Details of its construction are not provided in Taylor's report, but judging from photographs it was wood-framed with wood-panel walls. Windows and doors were blown out of the structure and it was filled with some centimeters of ash, but the walls and roof remained intact on most of the building. Taylor reports that the building was moved wholesale about 5 m in the down-flow direction, and that much of the damage on the up-flow face was due to 'flying debris'. Other buildings associated with the local administration were completely destroyed, leaving only their floors intact. It seems likely that the Commissioner's building would have been destroyed had it been firmly planted on a foundation and therefore had an immobile floor. Instead, much of the lateral load produced by the

PDC was taken up by motion of the whole structure. The three steel huts were partly collapsed. A steel-framed hospital was completely destroyed.

At Sangara Mission, near the distal end of the PDC, the degree of damage is somewhat less. Tree blowdown was not complete here. The major structures here were the mission house and a complex of sheds to the upstream side of the house (Fig. 14). Damage to these wood frame sheds included collapse of a few rooms and stripping of some roof and wall panels; however, judging from the photographs in the report of Taylor (1958), most of the wood frame of the sheds remained standing. The mission house, 10–20 m downstream, was largely undamaged except for some holes produced by flying rocks; even many of the windows remained intact.

This extent of damage suggests dynamic overpressures of 7–20 kPa ($\sim$ 1–3 psi) at Higaturu, and about 7 kPa at Sangara Mission. Taylor (1958) estimated the velocity of the PDC on 21 January 1951 to range from 27–93 m/s, based on distance covered and the duration of the explosive event as estimated by eye witnesses. Fig. 4 shows this range of conditions on the dynamic overpressure vs. flow speed diagram presented above, from which we can infer that the particle concentration of the PDC at these locations was between about 2×10^{-3} and 6×10^{-2}. These relatively low concentrations would be considered in the pyroclastic surge regime in past literature and are consistent with other observations at this site, such as the thickness of deposits here (centimeters to a few decimeters) and the proximity (< 2 km) to the distal singe zone where the current probably became buoyant. Taylor (1958) also used damage such as a bent flagpole to estimate flow velocities and arrived at a range of 70–80 m/s at Higaturu, but he did not account for the particle load of the PDC.

6.2. St. Pierre, Martinique, 1902

The 20 May 1902 nuees ardente erupted from Mt. Pelee destroyed the city of St. Pierre, Martinique (part of the city had been heavily damaged less than 2 weeks earlier, on 8 May, as well). Photographs taken by Lacroix shortly after these eruptions (Lacroix, 1904), show that practically no complete structures were left standing, although some individual walls remained standing. I have not been able to find any descriptions of the building types that dominated the city of Martinique, but it seems reasonable to assume (and also supported by photographs taken at the time) that most of the buildings in the city were masonry, but the degree of reinforcement is unknown. Based on the level of overall destruction, though, it seems that dynamic overpressures of 30 kPa and greater are likely. Because some walls were

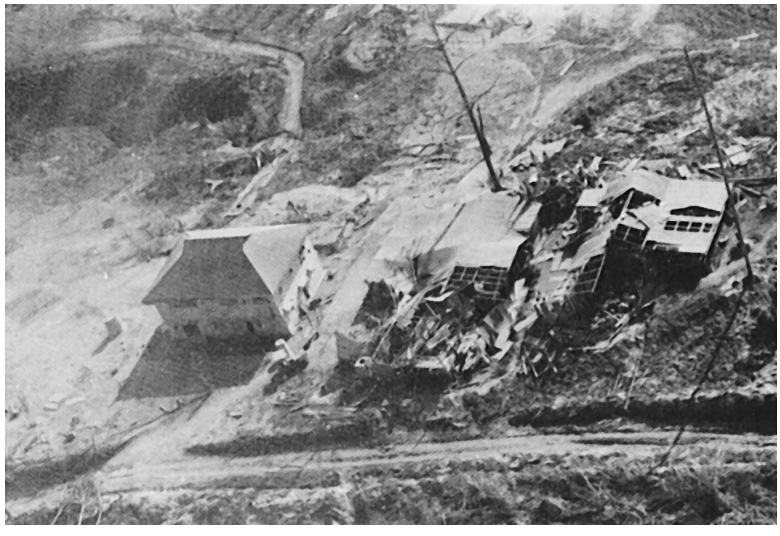

Fig. 14. Sheds and house at Sangara Mission damaged by pyroclastic density current from Mt. Lamington. Flow was from right to left. From Taylor (1958).

still standing, an upper bound on dynamic overpressure may be estimated at ~70 kPa, above which I think there would have been no remaining walls. Lacroix (1904) estimated velocities to range between 100–150 m/s for the 20 May event (see also Bourdier et al., 1989). Using these very crudely-derived bounds, I estimate that particle concentration in the PDC ranged from about 3×10^{-3} to 2×10^{-2} (Fig. 4). This range is consistent with that estimated by LaJoie et al. (1989), from 10^{-3} to about 5×10^{-2}, based on sedimentological arguments, and with the interpretations of Fisher et al. (1980), Fisher and Heiken (1982), Bourdier et al. (1989), Charland and LaJoie (1989); Boudon and LaJoie (1989).

6.3. Herculaneum, 79 AD

Sigurdsson et al. (1985) provide some information on the structural damage in Herculaneum that was caused by pyroclastic density currents from the 79 AD eruptions of Vesuvius. The first of these PDCs to affect Herculaneum (surge S-1 of Sigurdsson et al., 1985) was sufficiently strong to knock down the large colonnade and portico that surrounded the palestra. Bricks, roof tiles, and other building fragments were transported a few meters, but Sigurdsson et al. (1985) infer that most walls remained standing after the passage of S-1. Assuming that the buildings were all unreinforced masonry, this level of damage indicated dynamic overpressures within the range of approximately 10–20 kPa. Sigurdsson et al. (1985) estimate that the velocity of this PDC was on the order of 30 m/s. On Fig. 4 I have attempted to bracket the conditions of the S1 PDC, assuming the above range of dynamic overpressure and allowing for a velocity between 30 ± 20 m/s. The results indicate that the S1 pyroclastic density current ranged in particle concentration from about 10^{-2}–0.5. According to Sigurdsson et al. (1985) the basal layer of S1 is massive and poorly sorted, consistent with a relatively high concentration, while the upper layer is cross bedded, indicating relatively lower particle concentration. These features are consistent with the concentrations indicated in Fig. 4, which cover the transition between what would traditionally have been called pyroclastic surge and pyroclastic flow.

The next major PDC to hit Herculaneum left deposits identified as S2 by Sigurdsson et al. (1985); S2 was strong enough to complete the destruction of the town by knocking down remaining walls. I estimate that the dynamic overpressure for such damage was between 35–70 kPa. Based on the similarities between the S2 deposits and those of the 18 May 1980 blast at Mount St. Helens, Sigurdsson et al. (1985) estimated that the S2 pyroclastic density current had velocities of 100–200 m/s at Herculaneum. Using these estimates to bracket the PDC conditions (Fig. 4) we can infer particle concentrations of ~1.5 $\times 10^{-3}$ to 1.5×10^{-2}.

7. Conclusions

In this paper I have attempted to use nuclear weapon test data for estimating damage to structures from pyroclastic density currents, taking into account the limits in making an analogy between the two types of explosive events. There are two results that I hope will be produced by this paper. First, the damage patterns and criteria reviewed here should be used in concert with predictions of dynamic pressure within PDCs that are derived from multiphase numerical simulation. Ultimately, such approaches will account for a range of particle sizes and three-dimensional processes, therefore producing simulations that are close approximations to real pyroclastic density currents in nature. By overlaying simulations of eruptive scenarios onto geographic data that includes building locations, sizes, and construction types, one should be able to produce maps of predicted damage; the probabilistic damage criteria in Figs. 8–13 would be particularly useful for this. Such maps can aid in planning for mitigation and emergency response. Coupled with scenario probabilities, this approach will move us toward rigorous risk assessment for urban centers near explosive volcanoes.

There will be specific issues around individual volcanoes that require more detailed study within the framework that is provided in this paper. For example, if a city at risk contains a wide range of masonry building types, it may be necessary to further refine estimates of their vulnerability according to the details of their construction, moving beyond the qualitative, general information provided here. In situations like this, detailed modeling of dynamic pressure loading may be appropriate, using tools devel-

oped in the engineering community to study the effects of blast loading on individual structures (e.g., Stein et al., 1977; Beshara, 1994).

The second outcome should be more quantitative mapping of structural damage around historic or future eruptions, and the application of these data to constraining both the conditions within pyroclastic density currents and to further refine damage predictions. Workers in the field in the aftermath of an explosive eruption should add such data as building damage, percentages of damage for certain types of buildings, orientations and construction of buildings where possible. Combining such data with the data that are already collected by pyroclastic geologists and with modeling studies will further tighten our ability to predict and mitigate the effects of explosive eruptions.

Acknowledgements

This review has benefited from many conversations with Grant Heiken, who also shared his excellent library for this work and also reviewed the manuscript. The paper was sponsored by the Los Alamos National Laboratory's Urban Security project, with internal research funds.

References

Baer, E.M., Fisher, R.V., Fuller, M., Valentine, G.A., 1997. Turbulent transport and deposition of the Ito pyroclastic flow—determinations using anisotropy of magnetic susceptibility. J. Geophys. Res. 102, 22565–22586.

Baxter, P.J., 1990. Medical effects of volcanic-eruptions: 1. Main causes of death and injury. Bull. Volcanol. 52, 532–544.

Baxter, P.J., Gresham, A., 1997. Deaths and injuries in the eruption of Galeras Volcano, Columbia, 14 January 1993. J. Volcanol. Geotherm. Res. 77, 325–338.

Beshara, F.B.A., 1994. Modeling of blast loading on aboveground structures. 1. General phenomenology and external blast. Computers and Structures 51, 585–596.

Blong, R.J., 1984. Volcanic hazards. Australia Academic Press, 452 pp.

Boudon, G., LaJoie, J., 1989. The 1902 Peleean deposits in the Fort Cemetary of St. Pierre, Martinique: a model for the accumulation of turbulent nuees ardentes. J. Volcanol. Geotherm. Res. 38, 113–129.

Bourdier, J.L., Boudon, G., Gourgaud, A., 1989. Stratigraphy of the 1902 and 1929 nuee-ardente deposits, Mt. Pelee, Martinique. J. Volcanol. Geotherm. Res. 38, 77–96.

Bursik, M.I., Kurbatov, A.V., Sheridan, M.F., Woods, A.W., 1998. Transport and deposition in the May 18, 1980, Mount. St. Helens blast flow. Geology 26, 155–158.

Charland, A., LaJoie, J., 1989. Characteristics of pyroclastic deposits at the margin of Fond Canonville, Martinique and implications for the transport of the 1902 nuees ardentes of Mt. Pelee. J. Volcanol. Geotherm. Res. 38, 97–112.

Dobran, F., Neri, A., Macedonio, G., 1993. Numerical simulation of collapsing volcanic columns. J. Geophys. Res. 98, 4231–4259.

Dobran, F., Neri, A., Todesco, M., 1994. Assessing the pyroclastic flow hazard at Vesuvius. Nature 367, 551–554.

Druitt, T.H., 1992. Emplacement of the 18 May 1980 lateral blast deposit ENE of Mount St. Helens, Washington. Bull. Volcanol. 54, 554–572.

Fisher, R.V., 1990. Transport and deposition of a pyroclastic surge across an area of high relief: the May 1980 eruption of Mount St. Helens, Washington. Geol. Soc. Am. Bull. 102, 1038–1054.

Fisher, R.V., Heiken, G., 1982. Mt. Pelee, Martinique: May 8 and 20, 1902, pyroclastic flows and surges. J. Volcanol. Geotherm. Res. 13, 339–371.

Fisher, R.V., Smith, A.L., Roobol, M.J., 1980. Destruction of St. Pierre, Martinique, by ash-cloud surges, May 9 and 20, 1902. Geology 8, 472–476.

Fisher, R.V., Heiken, G., Hulen, J.B., 1997. Volcanoes, crucibles of change. Princeton Univ. Press, Princeton, 317 pp.

Freundt, A., Schmincke, H.-U., 1986. Emplacement of small-volume pyroclastic flows at Laacher See (East-Eiffel, Germany). Bull. Volcanol. 48, 39–59.

Giordano, G., Dobran, F., 1994. Computer-simulations of the Tuscolano-Artemisios 2nd pyroclastic flow unit (Alban Hills, Latium, Italy). J. Volcanol. Geotherm. Res. 61, 69–94.

Glasstone, S., Dolan, P.J., 1977. The effects of nuclear weapons. US Dept. of Defense and Dept. of Energy, 653 pp.

Hayen, C.L., 1952. Scientific director's report of atomic weapon tests at Einewetok, 1951: US Navy structures. Atomic Energy Commission Report WT-91.

Johnston, B.G., 1956. Damage to commercial and industrial buildings exposed to nuclear effects. Atomic Energy Commission Report WT-1189.

Kieffer, S.W., 1981. Fluid dynamics of the May 18, 1980 blast at Mount St. Helens. In: Lipman, P.W., Mullineaux, D.R. (Eds.), The 1980 Eruptions of Mount St. Helens, Washington. US Geological Survey Prof. Pap. 1250, pp. 401–420.

Lacroix, A., 1904. La Montagne Pelée et ses Eruptions. Masson et Cie, Paris, 662 pp.

LaJoie, J., Boudon, G., Bourdier, J.L., 1989. Depositional mechanics of the 1902 pyroclastic nuees-ardente deposits of Mt. Pelee, Martinique. J. Volcanol. Geotherm. Res. 38, 131–142.

Melosh, H.J., 1989. Impact Cratering, A Geologic Process. Oxford Univ. Press, New York, 245 pp.

Neri, A., Dobran, F., 1994. Influence of eruption parameters on the thermofluid dynamics of collapsing volcanic columns. J. Geophys. Res. 99, 11833–11857.

Neri, A., Macedonio, G., 1996. Numerical simulation of collapsing volcanic columns with particles of two sizes. J. Geophys. Res. 101, 8153–8174.

Palladino, D.M., Valentine, G.A., 1995. Coarse-tail vertical and lateral grading in pyroclastic flow deposits of the Latera Volcanic Complex (Vulsini, central Italy): origin and implications for flow dynamics. J. Volcanol. Geotherm. Res. 69, 343–364.

Pickering, E.E., Bockholt, J.L., 1971. Probabilistic Air Blast Failure Criteria for Urban Structures. Standford Research Institute, Menlo Park, CA.

Randall, P.A., 1961. Damage to conventional and special types of residences exposed to nuclear effects. Atomic Energy Commission Report WT-1194.

Shaw, E.R., McNea, F.P., 1957. Exposure of mobile homes and emergency vehicles to nuclear explosions. Atomic Energy Commission Report WT-1181.

Sigurdsson, H., Carey, S., Cornell, W., Pescatore, T., 1985. The eruption of Vesuvius in A.D. 79. Natl. Geographic. Res. 1, 332–387.

Sparks, R.S.J., 1976. Grain size variations in ignimbrites and implications for the transport of pyroclastic flows. Sedimentology 23, 147–188.

Sparks, R.S.J., 1986. The dimensions and dynamics of Plinian eruption columns. Bull. Volcanol. 48, 3–15.

Stein, L.R., Gentry, R.A., Hirt, C.W., 1977. Computational simulation of transient blast loading on 3-dimensional structures. Comp. Met. Appl. Mech. Eng. 11, 57–74.

Taylor, G.A.M., 1958. The 1951 Eruption of Mount Lamington, Papua. BMR Bulletin 38, 2nd edn., (published 1983), Australian Government Publishing Service, 129 pp.

Valentine, G.A., Wohletz, K.H., 1989. Numerical models of Plinian eruption columns and pyroclastic flows. J. Geophys. Res. 94, 1867–1887.

Valentine, G.A., Wohletz, K.H., Kieffer, S.W., 1991. Sources of unsteady column dynamics in pyroclastic flow eruptions. J. Geophys. Res. 96, 21887–21892.

Valentine, G.A., Wohletz, K.H., Kieffer, S.W., 1992. Effects of topography on facies and compositional zonation in caldera-related ignimbrites. Geol. Soc. Am. Bull. 104, 154–165.

Wilson, C.J.N., 1985. The Taupo eruption, New Zealand: II. The Taupo ignimbrite. Philos. Trans. R. Soc. London, Ser. A 314, 229–310.

Wohletz, K.H., McGetchin, T.R., Sandford, M.T. II, Jones, E.M., 1984. Hydrodynamic aspects of caldera-forming eruptions: numerical models. J. Geophys. Res. 89, 8269–8286.